7

Jennifer L. Sano, Ken T. Ratcliffe, and D.R. Spain, 2013, Chemostratigraphy of the Haynesville Shale, *in* U. Hammes and J. Gale, eds., Geology of the Haynesville Gas Shale in East Texas and West Louisiana, U.S.A.: AAPG Memoir 105, p. 137–154.

Chemostratigraphy of the Haynesville Shale

Jennifer L. Sano and Ken T. Ratcliffe

Chemostrat Inc, 5850 San Felipe, Suite 500, Houston Texas 77057, U.S.A. (e-mails: jjen1023@gmail.com; kenratcliffe@chemostrat.com).

David R. Spain

BP America, Inc., 501 Westlake Park Boulevard, Houston, Texas 77079, U.S.A. (e-mail: David.Spain@bp.com).

ABSTRACT

The Haynesville Shale, an Upper Jurassic (Kimmeridgian) age calcareous and locally organic-rich mudrock, is one of many prominent shale gas plays in North America. As shale plays increase in importance, the ability to define basin-wide, robust, and stable stratigraphic frameworks using data derived from well-bores becomes increasingly critical. Here, the technique of chemostratigraphy is used to define a stratigraphic framework that extends through ten wells ranging from eastern Texas to northwestern Louisiana.

Stratigraphic variations in inorganic geochemistry allow clear differentiation of Haynesville Shale from the underlying Smackover Formation, the Gilmer Lime, and the overlying Bossier Formation. More importantly, however, interpretation of the results allows two chemostratigraphic packages and four geochemically distinct units to be defined and correlated within the Haynesville Shale. The lithostratigraphic units are geochemically differentiated using variations in SiO_2, Al_2O_3, MgO, Zr, and Nb, whereas the units within the Haynesville Shale are defined using changes in CaO, Al_2O_3, MgO, Fe_2O_3, Rb/K_2O and Th/U values, and V enrichments. By integrating the geochemistry with x-ray diffraction and total organic carbon (TOC) results, it becomes apparent that the driving forces behind the changing geochemistry within the Haynesville Shale are the amounts of anoxia in the lower portion of the Haynesville Shale and of CaO input in the upper portion.

Cyclical fluctuations in the relative abundances of Zr and Nb are interpreted to represent transgressive—regressive cycles—and provide enhanced correlation within the Haynesville Shale. By combining stratigraphic changes in Zr/Nb values with V enrichments, it is shown that the most severe period of anoxia is associated with the transgressive portion of the oldest cycle. Importantly, this suggests that this stratigraphic horizon is where maximum TOC can be expected. Lateral changes in geochemistry within the Haynesville Shale demonstrate that terrigenous input was highest in the northwest sector of the basin, primarily in East Texas, and anoxia was greatest in the east of the basin, primarily in Louisiana.

DOI: 10.1306/13441847M1053602

INTRODUCTION

Shale gas plays have become increasingly important in North America over the past decade, with production growing to more than 8bcfd (billion cubic feet per day) in 2009 (Stevens and Kuuskaraa, 2009). The Upper Jurassic (Kimmeridgian) Haynesville Shale is one of the most important plays, with estimated recoverable reserves up to 100 TCF (Spain and Anderson, 2010). Technological improvements in horizontal drilling, hydraulic fracturing, and completion technology have made it possible to unleash this formation's potential, as well as that of other shale plays. Along with the development of what are traditionally termed "unconventional" plays, the need for unconventional methodologies for stratigraphic correlation has also developed. Because mudrocks are particularly difficult to characterize given their macroscopic homogeneity, mineralogic complexity, and limited availability of biostratigraphic constraints, additional techniques are needed to complement traditional analytical methods (Wright et al., 2010b). Although homogenous on the macro scale, mudrocks possess considerable variation in their geochemistry on a smaller scale, which is why the inorganic geochemistry of organic-rich mudrocks has routinely been used to help elucidate paleoredox conditions during oceanic anoxic events (e.g., Tribovillard et al., 2006; Turgen and Brumsack 2006; Tribovillard et al., 2008; Negri et al., 2009; Jenkyns, 2010).

Additionally, the petroleum industry has made use of inorganic whole-rock geochemical data to define stratigraphic correlations for over a decade (Hildred et al., 2010; Ratcliffe et al., 2010; Wright et al., 2010a). Published accounts using the chemostratigraphic approach are largely focused on fluvial successions, where traditional stratigraphic correlation techniques are often problematic (e.g., Pearce et al., 2005; Ratcliffe et al., 2006; Hildred et al., 2010; Ratcliffe et al., 2010; Wright et al., 2010a). The chemostratigraphic technique relies on recognizing changes in element concentrations through a section and using those to develop a stratigraphic characterization that is based on changes in geological features, such as paleoclimate (Pearce et al., 2005, Ratcliffe et al., 2010) and provenance (Ratcliffe et al., 2007, Wright et al., 2010).

Here, we combine the approaches of chemostratigraphic and oceanic anoxic event workers and apply them to ten wells drilled in the Upper Jurassic Haynesville/Bossier area in eastern Texas and northwestern Louisiana (Figure 1). This enables definition of a robust, repeatable, nonsubjective correlation framework in which the defined chemostratigraphic packages largely correspond to lithostratigraphic units. Within the chemostratigraphic package framework, we refine the internal stratigraphy of the Haynesville Shale, using a traditional chemostratigraphic approach of defining geochemical units (see Ratcliffe et al., 2010 and references cited therein). Additionally, cyclical variations in selected element ratios are used for correlation and are interpreted to represent base-level fluctuations. The same geochemical data used for stratigraphic interpretations (see Rowe and Manali, this volume) are used to identify areas in the basin that received highest terrigenous input, the parts of the basin that suffered most severe anoxia. We end with a discussion of how the most severe anoxia observed throughout the basin may be associated with transgressive sequences.

Materials

A total of 1421 core samples from 10 wells distributed throughout the east Texas/west Louisiana Haynesville/Lower Bossier area were analyzed for this study (Table 1). The wells are CGU 13 17, Watson 4, Williams 22 3, Glaspie Ocie GU 10, Georgetown 885 2, George T W GU A-8H, Martin R O Minerals 23, Hall 5 1, Elm Grove Plantation 63, and Johnson Trust 1 2H Pilot, all located in eastern Texas and western Louisiana (Figure 1). The Williams 22 3 and Martin R O Minerals 23 wells were combined to make one composite well. An additional 10 cutting samples were used to fill in an area of the Johnson Trust well where core was sparse. Core samples were analyzed at approximately 2 ft (0.6 m) intervals, and cutting samples were recovered at 30 ft (9.1 m) intervals.

A subset of samples from four of the wells in this study were analyzed by XRD to determine their bulk mineralogy (Table 1). The procedure followed published protocols (Pearce et al., 2005; Ratcliffe et al., 2006; Ratcliffe et al., 2007; Ellwood et al., 2008). X-ray diffraction (XRD) mineralogical data allow a better understanding of the relationship between the whole rock geochemistry and the mineralogy, discussed in the "Geochemistry and Mineralogy" section later.

Methodology

Chemostratigraphy, as applied in this study, is a method that uses major and trace element geochemistry for the characterization and correlation of strata. The elemental data for the paper were acquired using inductively coupled plasma optical emission spectrometry (ICP OES) and inductively coupled

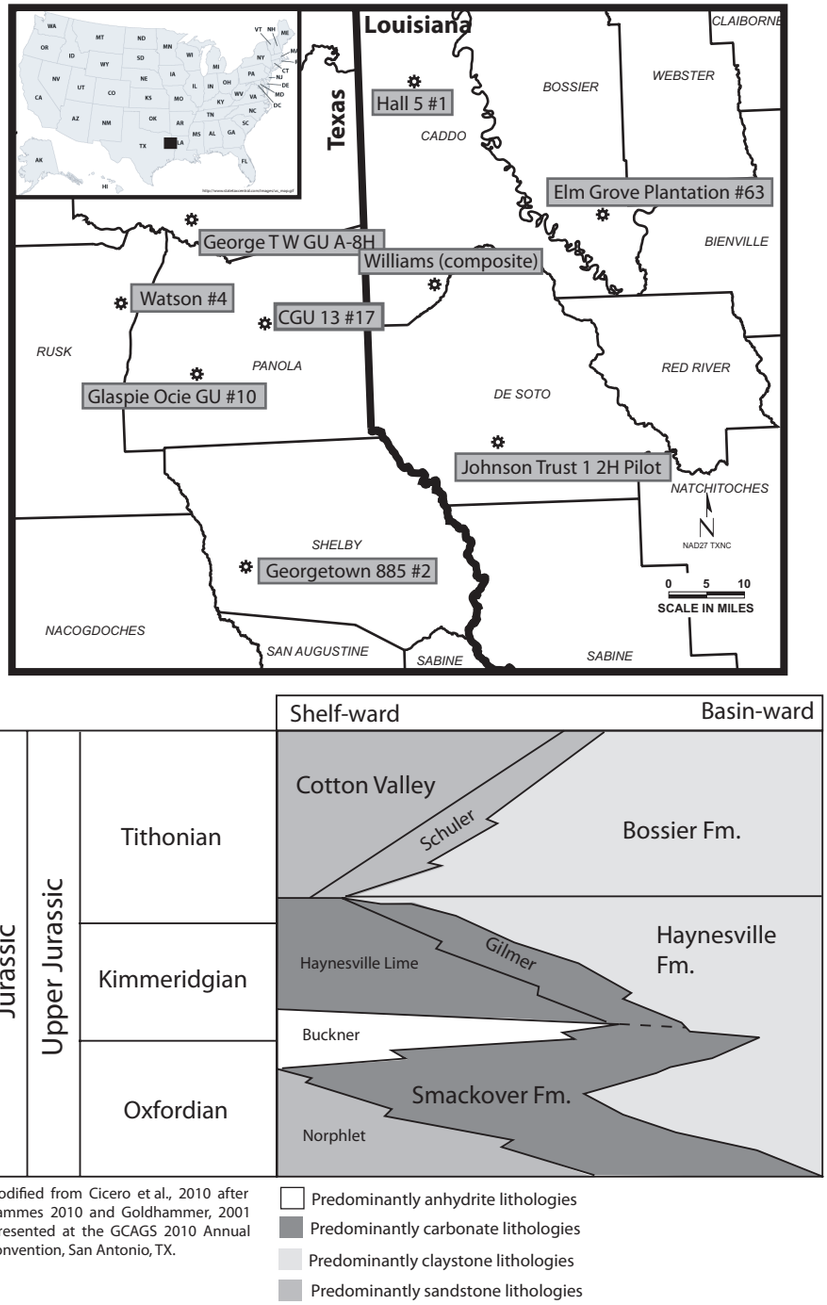

Figure 1. Map (top) showing the location of the wells in this study. They are: CGU 13 17, Watson 4, Williams 22 3, Glaspie Ocie GU 10, Georgetown 885 2, George T.W. GU A-8H, Martin R O Minerals 23, Hall 5 1, Elm Grove Plantation 63, and Johnson Trust 1 2H Pilot, all located in eastern Texas and western Louisiana. Wells Williams 22 3 and Martin R O Minerals 23 were combined to make one composite well and are listed as Williams (composite) on the map. The stratigraphic column (bottom) shows the succession of formations encountered in this study. 5 mi (8.04 km).

plasma mass spectrometry (ICP MS) as well as x-ray fluorescence (XRF) spectrometry.

Samples were prepared for ICP analysis using a Li-metaborate fusion (Jarvis and Jarvis, 1995). ICP OES and MS provide data for 50 elements (10 major elements, reported as oxide percent by weight [SiO_2, TiO_2, Al_2O_3, Fe_2O_3, MgO, MnO, CaO, Na_2O, K_2O, and P_2O_5]; 25 trace elements, reported as parts per million [Ba, Be, Bi, Co, Cr, Cs, Cu, Ga, Hf, Mo, Nb, Ni, Pb, Rb, Sn, Sr, Ta, Tl, Th, U, V, W, Y, Zn, and Zr]; and 14 rare earth elements [REE], reported as parts per million [La, Ce, Pr, Nd, Sm, Eu, Gd, Tb, Ho, dy, Er, Tm, Yb, and Lu]). Precision error for the major element data is generally better than 2% and is around 3% for the high abundance trace element data derived by ICP OES (Ba, Cr, Sc, Sr, Zn, and Sr). The remaining trace

Table 1. Study interval depths (in MD) and number of samples analyzed from each well.

Well	Study Interval (ft.)	Total No. of Feet	Cutting Samples	Core Samples	Total	XRD Samples
CGU 13 17	10,471-10,777	306	0	120	**120**	**161**
Watson 4	11,142-11,489	347	0	184	**184**	**22**
Williams 22 3	11,537-11,755	218	0	104	**104**	**0**
Glaspie Ocie GU 10	10,624-10,872	248	0	114	**114**	**22**
Georgetown 885 2	11,650-12,089	439	0	129	**129**	**58**
TW George A-8H	10,887-11,356	469	0	277	**277**	**48**
R O Minerals 23	11,080-11,341	261	0	67	**67**	**0**
Hall 5	10,146-10,486	340	0	179	**179**	**0**
Elm Grove Plantation 63	11,015-11,191	176	0	84	**84**	**28**
Johnson Trust	11,182-11,891	709	10	163	**173**	**0**
		Totals	**10**	**1421**	**1431**	**339**
			Total no. of samples			**1431**

elements are determined from the ICP MS and data are generally less precise, with precision error on the order of 5%. Accuracy error is +− 1% for majors and +−3−7 ppm for trace elements depending on abundance. Expanded uncertainty values (95% confidence) that incorporate all likely errors in a statistical framework derived from 11 batches of five certified reference materials (CRMs), each prepared in duplicate, are typically 5–7% (relative) for major elements and 7–12% (relative) for trace elements. The ICP OES and MS facility that produced the data presented here was granted laboratory quality system accreditation to ISO 17025:2005, which is equivalent to the ISO 9000 series but focused on laboratory total quality systems.

To obtain S data, samples were analyzed using a Spectro Xepos Energy Dispersive–X Ray Fluorescence (ED-XRF) system. Sample preparation was pressed powder pellet sample. Calibrations are bespoke, developed in-house by Chemostrat to provide data from organic-rich mudstones. For data quality control and drift correction on the ED-XRF, every eighth sample analyzed is an in-house standard, which in this case was Monument Slate. Additionally, comparisons with ICP data provided a secondary check on XRF data quality for major element concentrations.

Although data for more than 50 elements are acquired as a result of these analyses, chemostratigraphic characterization typically uses a relatively small number of elements or ratios of elements (Pearce et al., 2005; Ratcliffe et al., 2006). The key elements and element ratios, termed key indices, are the foundation for constructing a chemostratigraphic zonation scheme, which is typically hierarchical. In this paper, the following chemostratigraphic hierarchy is applied:

1) Package: An interval whose mudstone geochemical composition can be differentiated from others in the study intervals.
2) Unit: An interval whose mudstone geochemistry allows it to be differentiated from others in its parent package. These are numbered to reflect their parent package, with, for example, Unit 4.1 being the oldest subdivision of Package 4, and 4.4 the youngest subdivision of that package.

CHEMOSTRATIGRAPHIC CHARACTERIZATION

Geochemical Characterization of Lithostratigraphic Units

Lithostratigraphic schemes can often be confused, with multiple names for the same unit being commonplace. In the area of this study there is confusion in the terminology of the "Haynesville" and "Bossier." Chemostratigraphy provides a nonsubjective means to differentiate lithostratigraphic units. The whole-rock geochemistry of a sedimentary deposit is largely controlled by its mineralogy and because different lithostratigraphic units are, by definition, composed of different relative percentages of minerals or different grain sizes of the same minerals, it therefore follows that lithostratigraphic units should have unique geochemical signatures. Using such unique geochemical signatures, the study interval was divided into five main chemostratigraphic packages, which correspond to four lithostratigraphic units: Package 1 (the Smackover Formation), Package 2 (the Gilmer Lime), Packages 3 and 4 (the Haynesville Shale) and Package 5 (the Bossier Formation) (Figures 2 and 3).

Smackover Formation (Package 1)

The Smackover Formation is a Late Jurassic limestone that is underlain by the Norphlet Formation and directly overlain by the Gilmer Lime (Cicero et al., 2010). Package 1 corresponds to part of the Smackover Formation. This package occurs at the base of the study interval, has very high CaO and low Al_2O_3 values resulting in a high CaO/Al_2O_3 ratio. The top of the Smackover Formation is geochemically defined by an upward decrease in CaO/Al_2O_3 values (Figure 2).

Gilmer Lime (Package 2)

The Gilmer Lime consists of backstepping carbonate facies (Cicero et al., 2010) and contains dark gray to brown micritic limestone and thin beds of dark gray

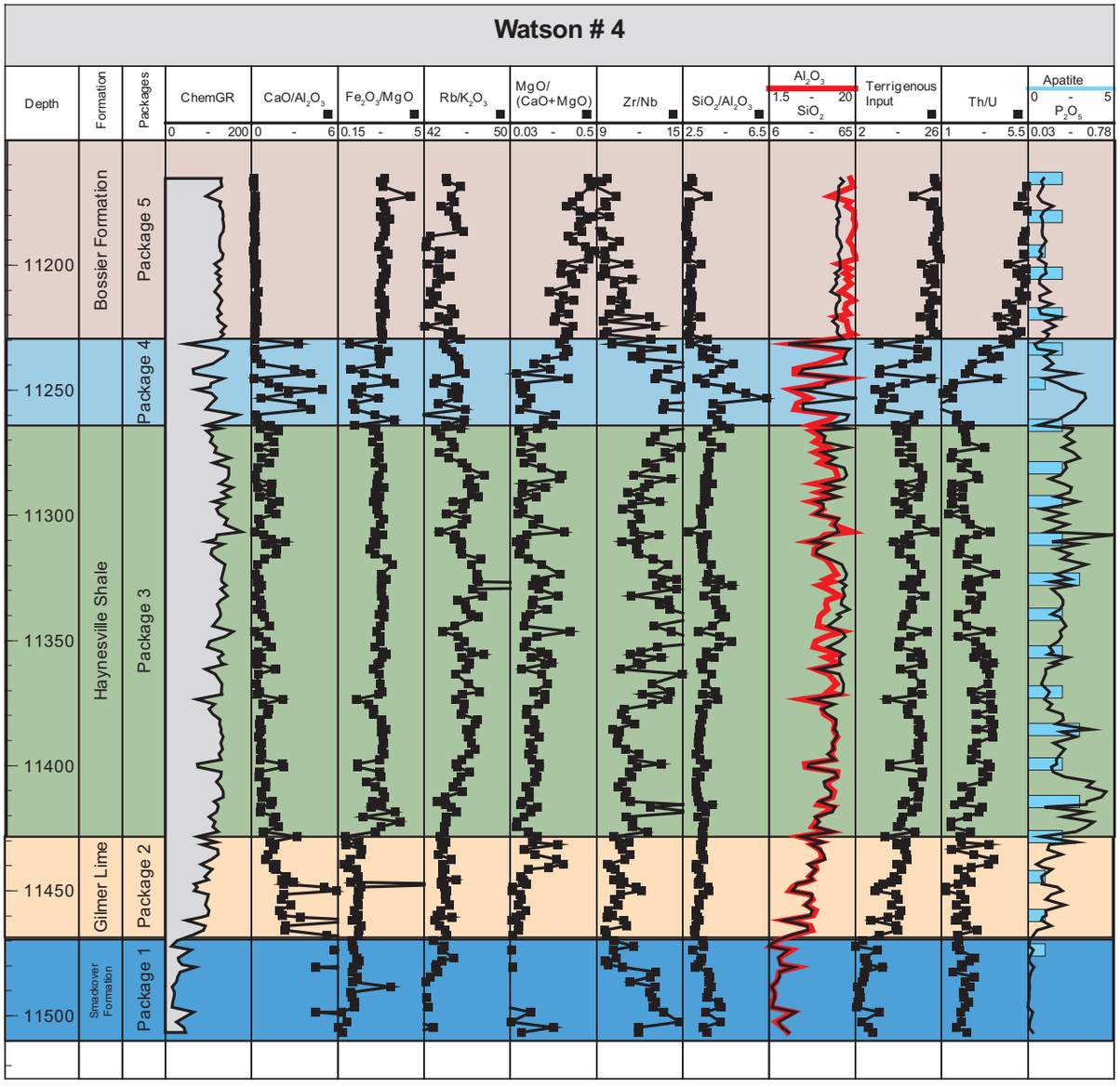

Figure 2. Watson 4 well as a type well showing the four main lithostratigraphic units: the Smackover Formation (Package 1), the Gilmer Lime (Package 2), the Haynesville Shale (Packages 3 and 4) and the shales of the Bossier Formation (Package 5). Black squares indicate sample locations and are omitted from the SiO_2, Al_2O_3 and P_2O_5 logs for clarity. The apatite contents, displayed as a bar chart in the right hand track, were determined by X-ray diffraction. ChemGR is derived from K, Th, and U values of the samples, using an algorithm to covert those values in API values.

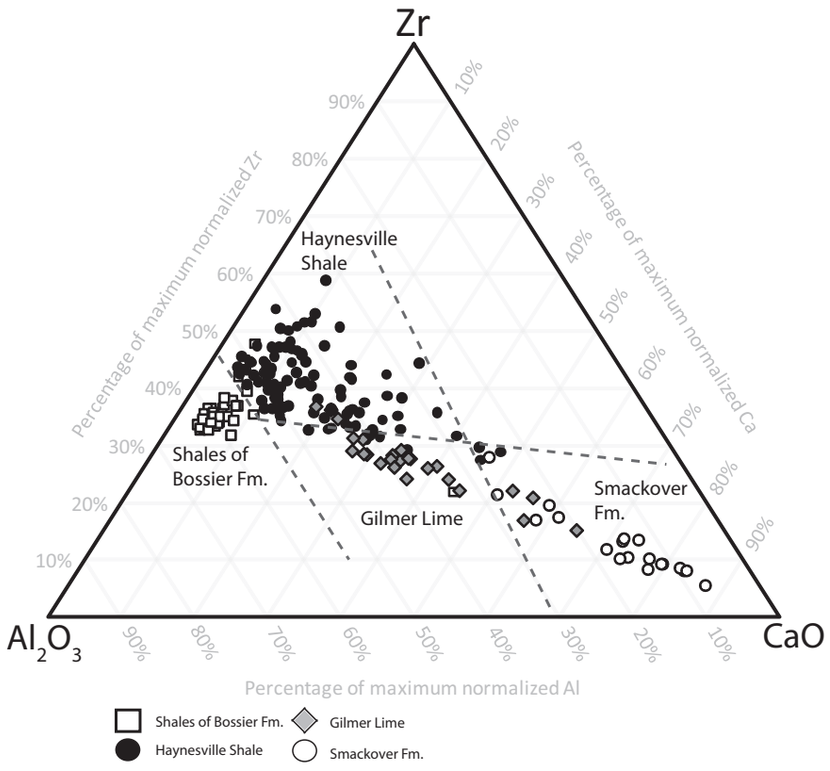

Figure 3. Ternary diagram showing the geochemical characterization of four main lithostratigraphic units in the Watson 4 well (see Figure 2 for chemical logs) based on variations in the amount of Al_2O_3, CaO, and Zr.

shale (Forgotson and Forgotson 1976). This limestone underlies the Haynesville Shale and overlies the Smackover Formation (Figure 1).

Package 2 is equivalent to the Gilmer Lime. Chemically, it appears as a transitional interval between the underlying and overlying sediments. It sees a gradation from an argillaceous carbonate at the bottom of the package to a calcareous claystone toward the top. The package is recognized by upwardly decreasing CaO/Al_2O_3 values (Figure 2). The top of the Gilmer Lime/Package 2 is geochemically identified by an upward decrease in CaO/Al_2O_3 values and an upward increase in Fe_2O_3/MgO values (Figure 2). An upward increase in Rb/K_2O values is also observed near this boundary in most wells.

Haynesville Shale

The Late Jurassic Haynesville Shale is a black, organic rich calcareous mudstone that was deposited under arid climatic conditions in a restricted intrashelf basin on the evolving Gulf Coast passive margin (Hammes et al., 2010). The Haynesville Shale is underlain by the Gilmer Lime and overlain by the Bossier Formation (Figure 1).

Packages 3 and 4 are equivalent to the Haynesville Shale. Package 3, which corresponds to the bulk of the Haynesville Shale, is recognized by low CaO/Al_2O_3 values, intermediate and upward increasing Rb/K_2O values, low to intermediate Th/U values and high Fe_2O_3/MgO values. Package 3 also has higher MgO/(CaO+MgO) values than underlying packages (Figure 2).

Package 4 is a relatively thin package that forms the top of the Haynesville Shale. Gradual changes in Zr/Nb and Th/U values from base to top of the package result in it being a somewhat transitional unit between Packages 3 and 5. Although transitional, the package does have higher CaO/Al_2O_3 and lower Fe_2O_3/MgO values than both the lower portion of the Haynesville Shale and the overlying Bossier Formation (Figure 2).

The top of the Haynesville Shale (top of Package 4) is recognized by a significant upward decrease in Zr/Nb values and a significant upward increase in Th/U and MgO/(CaO+MgO) values. An upward decrease in CaO/Al_2O_3 values is also observed at the Haynesville Shale/Bossier Formation boundary.

Shales of the Bossier Formation

The Late Jurassic Bossier Formation overlies the Haynesville Shale (Cicero et al., 2010) (Figure 1). The shales of the Bossier Formation have lower CaO values and higher amounts of clay than the underlying Haynesville Shale.

Package 5 corresponds to shales from the Bossier Formation. It has higher MgO/(CaO +MgO) values and lower amounts of CaO. The package also is characterized by high Th/U values compared to the underlying Haynesville Shale. The package also has very low Zr/Nb values (Figure 2).

Geochemical Definition of Interformational Units

Chemostratigraphy typically provides a means to refine correlations beyond what is possible lithostratigraphically (Pearce et al., 2005; Ratcliffe et al., 2006; Hildred et al., 2010). Using a classical chemostratigraphic approach (as typified by Ratcliffe et al., 2010) enables four geochemical units to be defined within Package 3, the Haynesville Shale, based mainly on changes in CaO, Al_2O_3, Th/U, and the enrichment factor of vanadium (EFV = $(V/Al_2O_3)_{sample}$ / $(V/Al_2O_3)_{average\ shale}$) (Figure 4).

Unit 3.1 is the youngest unit in the Haynesville Shale. It is characterized by higher EFV and lower Th/U values than Unit 3.2. It also has higher CaO /Al_2O_3 and Fe_2O_3/MgO values and lower Rb/K_2O and Th/U values than Unit 3.2.

Unit 3.2 is differentiated from Unit 3.1 by higher Th/U and lower EFV values, and from Unit 3.3 by its lower CaO/Al_2O_3 values.

Unit 3.3 is characterized by its higher CaO/Al_2O_3 values than Units 3.2 and 3.4.

Unit 3.4 is characterized by lower CaO/Al_2O_3 values than Unit 3.3.

To understand the geological significance of the key element ratios used to define the chemostratigraphic packages and geochemical units, the geochemistry needs to be linked to mineralogy.

GEOCHEMISTRY AND MINERALOGY

The chemostratigraphic characterization shown in Figures 2, 3, and 4 is based on selected key elements and ratios, as described previously. The next step in a chemostratigraphic study is to develop a geologic interpretation and stratigraphic scheme based on the correlation. To do so, an understanding of the mineralogical controls on the key elements is needed.

The most pragmatic way to determine the basic mineralogical controls is to directly compare the geochemical data acquired from a sample with the mineralogical data acquired from that same sample. Figure 5 shows mineralogical data obtained by XRD analysis compared to key elements and ratios obtained by ICP analysis for the Carthage CGU 13 17 well. Looking at this comparison, it becomes apparent that:

- Al_2O_3 concentrations are related to the amount of clay
- SiO_2 concentrations are related to the amount of detrital quartz and clay
- Th concentrations are related to the total clay contents
- SiO_2/Al_2O_3 values are related to the quartz/clay ratio
- CaO concentrations are related to amount calcite
- Na_2O concentrations are related to the amount of plagioclase
- MgO shows a relationship to both the amount of chlorite and the amount of dolomite. Typically, where dolomite contents are low, the MgO chemical log follows the chlorite distribution; but where dolomite is high, the MgO chemical log follows the dolomite abundance.
- Fe_2O_3/MgO is a key element ratio and in Figure 5 its distribution clearly mimics the pyrite contents. Although the exact reasons for this relationship cannot be proved, it is suggested that since they are both components of chlorite, whereas pyrite contains no MgO, the ratio is highlighting Fe_2O_3 associated with pyrite.
- U, S, and EFV all display high values in intervals where TOC is high, that is, display a broad association, but the relationships between these three variables and TOC are not as well developed as the relationship between elements and mineralogy described previously (Figure 5).

Principal Components Analysis (PCA)

The direct comparison of elemental and mineralogical data described above provides a basic understanding of which minerals are controlling some elements and element ratios. This understanding can be enhanced by using principal components analysis (PCA). PCA is used in many chemostratigraphic studies (Pearce et al., 2005; Svendsen et al., 2007; Ellwood et al., 2008; Pe-Piper et al., 2008) to determine how elements are associated with one another in the study interval. By using XRD to understand element-mineral associations, and PCA to understand element-element associations, it becomes possible to suggest mineralogical controls on key elements and element ratios used to devise the chemostratigraphic zonation.

PCA reduces the total variation in a dataset, which in this case are the element concentrations, to a smaller

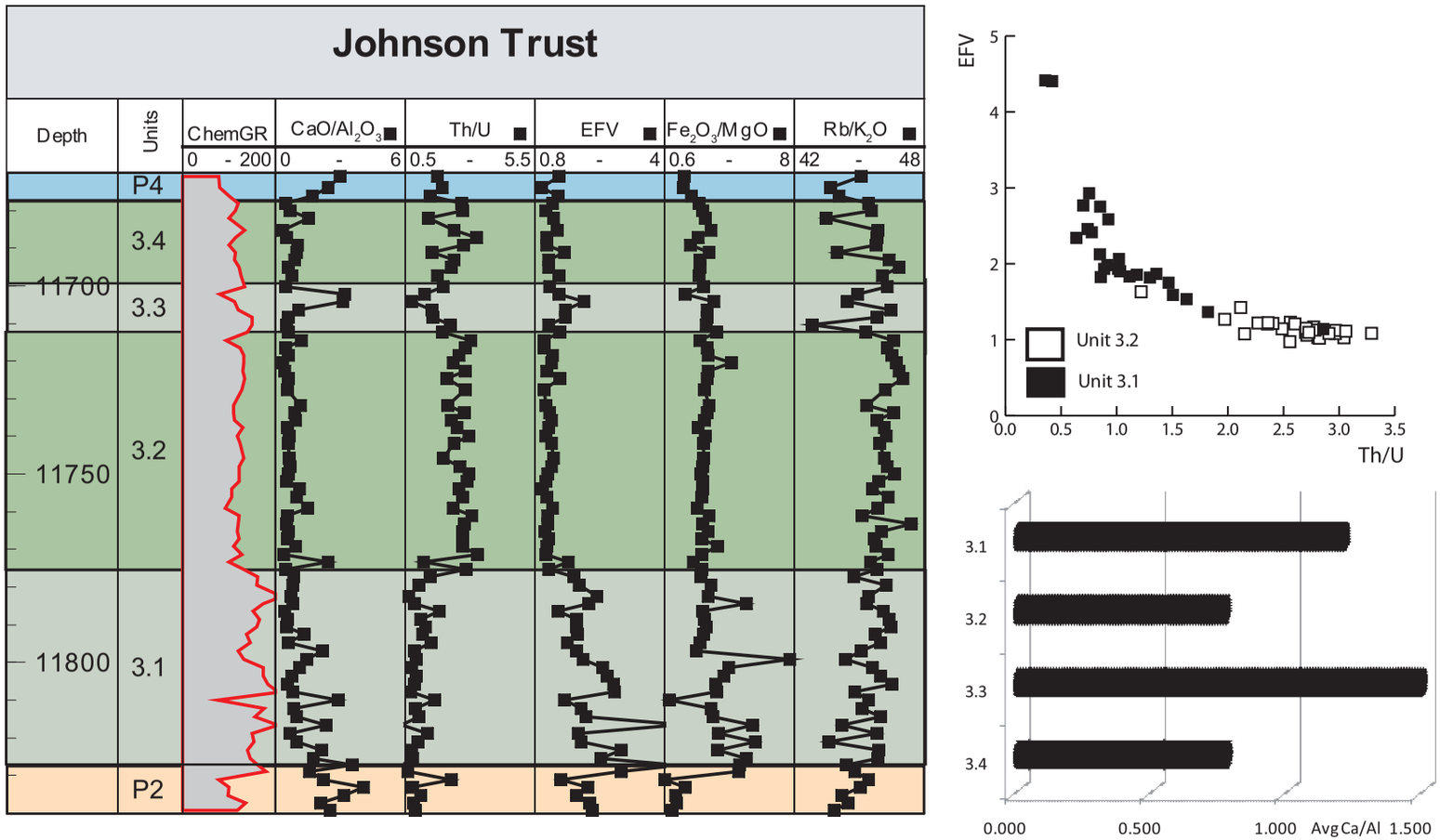

Figure 4. Key geochemical logs showing the chemical variations in Units 3.1–3.4 defined within the Haynesville Shale. The units are differentiated based on the average CaO/Al_2O_3 values (bar graph), whereas Units 3.1 and 3.2 are also differentiated based on the enrichment factor of vanadium (EFV= $(V/Al_2O_3)_{sample}$ / $(V/Al_2O_3)_{average\ shale}$) and Th/U values (binary diagram).

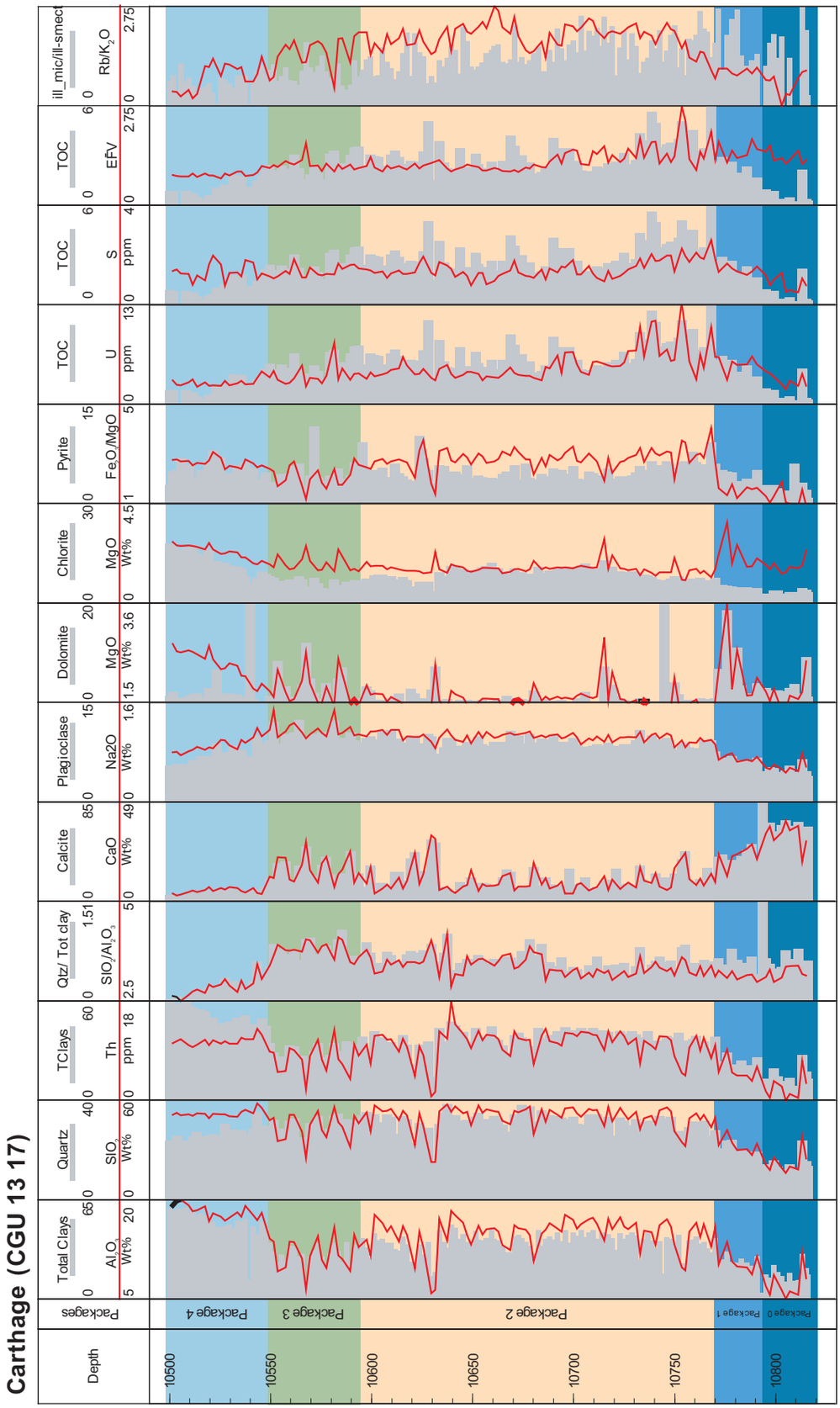

Figure 5. Comparison of selected mineralogical data and total organic carbon (TOC) data with selected geochemical variables.

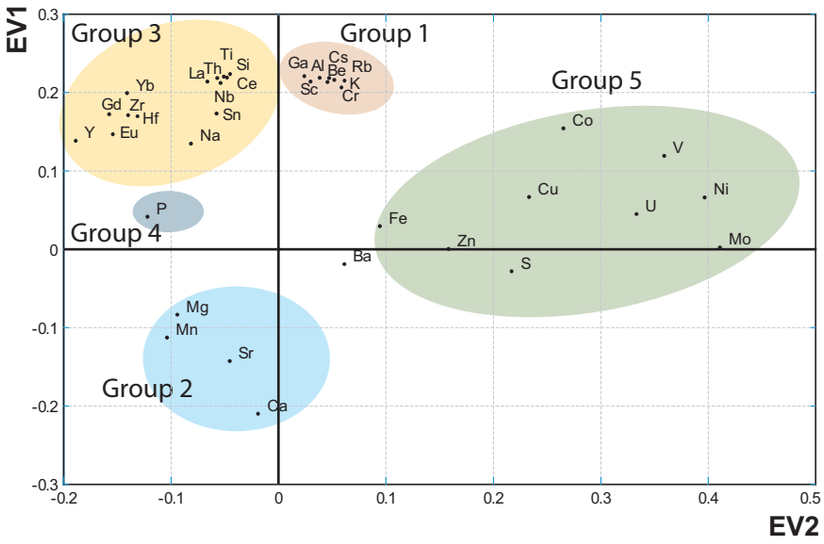

Figure 6. Eigenvector (EV) cross plots for data derived by principal components analysis (PCA) of geochemical data of samples from Packages 1, 2, and 3 in all wells described in this study. All elements have been abbreviated such that Al = Al_2O_3.

number of variables termed principal components (PC) (Shaw, 2003). A principal component score is assigned to each sample as determined from the eigenvector (EV). The EVs are then plotted against each other, and the closer the variables (elements) plot to one another, the more closely associated they are to one another in the sample suite.

Figure 6 summarizes the results of PCA carried out on geochemical data acquired from Packages 2, 3, and 4. Fifty-three percent of the variation in the dataset is accounted for by principal components 1 and 2. Package 1, a carbonate-rich package, and Package 5, which has a strong siliciclastic component, have not been used in the statistical analysis to focus on the Haynesville Shale itself and eliminate any skewing of the data. Five broad groupings can be recognized as follows:

Group 1 includes Al_2O_3, Be, Cr, Cs, Ga, K_2O, Rb, and Sc. As shown in Figure 5, Al_2O_3 is related to clay minerals; therefore, elements associated with Al_2O_3 are likely to be primarily controlled by clay mineral distribution.

Group 2 includes CaO, MgO, MnO, and Sr. Because CaO is associated with calcite (Figure 5), it is likely that the other elements in this group are also associated with carbonates.

Group 3 includes SiO_2, Cs, Gd, Hf, La, Lu, Na_2O, Nb, Sn, Th, TiO_2, Y, Yb, and Zr. This group plots close to Group 1 elements because the component elements are also associated with terrestrially derived minerals. However, they do form a separate cluster and typically SiO_2 is associated with the amount of silt-size quartz in a silty claystone (Pearce et al., 2005; Ratcliffe et al., 2006; Ratcliffe et al., 2010). Zr and Hf are associated with detrital zircon, which is typically present in silty claystones as fine sand or silt-sized particles, such as opaque and heavy minerals. Na_2O, as demonstrated by comparison with XRD data (Figure 5), is associated with plagioclase feldspar. Therefore, elements in this group are associated with coarser fraction of terrigenous material in the silty claystones.

Group 4 includes only P_2O_5, which has been shown by comparison with XRD data to be related to apatite (Figure 2). Although it cannot be determined geochemically if this is detrital or biogenic apatite, the fact that P_2O_5 plots on its own instead of with the Group 3 detrital elements indicates a biogenic source.

Group 5 includes Ba, Co, Cu, Fe_2O_3, Mo, Ni, U, V, and Zn. U is shown on Figure 5 to be broadly associated with TOC and therefore elements in this group can be expected to somehow be related to organic matter or minerals developed in association with high organic matter contents. V, Co, Mo, and Ni are all redox sensitive elements that tend to be more soluble under oxidizing conditions and less soluble under reducing conditions, resulting in authigenic enrichments in oxygen-depleted sedimentary facies (Tribovillard et al., 2006), that is, facies likely to have high TOC contents. The presence of Fe_2O_3, Zn, and Cu in this group probably reflects the influence of pyrite, an authigenic mineral associated with anoxia or euxinia.

KEY ELEMENTS AND RATIOS: SUMMARY

By combining the results of visual comparison of elements and element ratios with selected mineralogical variables with the results of PCA, the following interpretations can be made for the elements used to chemostratigraphically characterize the study intervals.

CaO/Al_2O_3: Indicates the weight percentage of calcite relative to the weight percentage of clay minerals.

Th/U: Kimura and Watanabe (2001) argue that Th/U values of less than 2 are associated with highly anoxic conditions and Th/U values over 8 are affiliated with oxic conditions. Here, Th is shown to be associated with clays and heavy minerals (Figures 5, 6), that is, the concentration of Th is primarily controlled by the amount of terrestrial input. U as demonstrated previously (Figures 5, 6) is associated with TOC and with elements that are enriched in anoxic sediments. Therefore, this ratio here is reflecting the amount of terrigenous material in the sediment versus the amount of organic matter in the sediment.

EFV (enrichment factor of vanadium): V is an element that is readily enriched in anoxic sedimentary facies (Tribovillard et al., 2006). In the PCA analyses (Figure 6), V is associated with other elements whose concentrations are potentially enriched in oxygen-depleted sedimentary facies. To demonstrate the degree of enrichment, the enrichment factor is calculated, where EFV = $(V/Al_2O_3)_{sample}$ / $(V/Al_2O_3)_{average\ shale}$. Enrichment factor values of 1 indicate average shale deposited in oxic environments, and values over 1 indicate enrichments because of deposition in oxygen-depleted environments. Therefore, EFV is a proxy for periods and severity of anoxia, which is supported in Figures 5 and 7, where EFV is shown to be related to TOC values.

Zr/Nb: Zr is typically associated with silt-grade detrital zircons in silty claystones, which is supported by its position on Figure 6 and its linear association with SiO_2 on Figure 8. Nb, when it plots in association with Zr and Hf on EV plots and displays a linear association with Zr and SiO_2 (Figure 8), is largely associated with Ti-oxide heavy or opaque minerals, such as rutile (Pearce et al., 2005). The Zr/Nb ratio, therefore, is indicative of subtle changes in the heavy mineral/opaque mineral content of the silty claystones. As discussed later, cyclical fluctuations in this ratio appear to be correlative between wells, but the exact controls on the ratio can only be hypothesized, as follows. SiO_2/Al_2O_3 values, when plotted as chemical logs display a marked similarity with Zr/Nb logs (Figure 2) and the two variables display a high R^2 value (0.81) (Figure 8), which implies that the two are linked in some way. SiO_2/Al_2O_3 is an indicator of the amount of quartz grains versus clay minerals (Figure 5) and is therefore typically an indicator of grain size in silty claystones. This implies that high Zr/Nb values are associated with coarser grained sediments and lower Zr/Nb values with finer grained sediments. No published accounts can be found that suggest zircon and Ti-oxide heavy minerals have naturally different grain size and the density of the grains isn't markedly different (Morton, personal communication). However, the Zr/Nb ratio is varying in proportion to grain size in the study interval here. In organic-rich black shales in general, it may be a more reliable grain-size indicator than SiO_2/Al_2O_3 because the numerator element can be linked to biogenic quartz.

Fe_2O_3/ MgO: As shown in Figure 5 and discussed above, this ratio mimics pyrite abundance. An increase in this ratio is used to define the boundary between Package 2 and Package 3 (the Gilmer Lime/Haynesville Shale boundary).

Terrigenous Input (Al_2O_3 + K_2O + TiO_2): These three elements are all closely associated in the sediment, with R^2 values above 0.88 for all three elements. They are therefore interpreted to be an indicator of total terrestrial sediment; therefore the sum of these elements gives an indication of the amount of terrigenous input into the basin (Pearce et al., 2005).

Rb/ K_2O: Although these elements are associated with clay-grade terrestrial detritus (Pearce et al., 2005), they are also both present in K-feldspar. The Rb/K_2O ratio in feldspar is lower than it is in clay minerals, which typically results in this ratio being a sensitive indicator of the amount of feldspar present (Ratcliffe et al., Ellwood et al., 2008). However, because K-feldspar contents are low in the Haynesville Shale, this ratio is likely indicating changes in the type of clay minerals present. This is tentatively supported on Figure 5, where Rb/K_2O displays a similar distribution to the variables illite/smectite and illite/mica, as determined by XRD, normalized against one another. Additional clay analyses, outside the scope of this paper, would be required to fully comprehend the controls on Rb/K_2O.

GEOCHEMISTRY AND TOTAL ORGANIC CARBON (TOC)

Typically in organic-rich shales, TOC displays a close linear relationship to U (Wright et al. 2010b). A broad association between U, S, and V is demonstrated in Figure 5, but Figure 7 demonstrates that the relationship between TOC and U is not that clearly developed, nor is the relationship with TOC and S. In some wells, for example, Carthage, there is a relationship developed; whereas in others, such as Elm Grove Plantation,

the relationship between TOC and the concentrations of U and S is not developed (Figure 5). In other words, the relationship between organic carbon and geochemistry is not a simple one, apparently showing lateral variations across the study area. Although undoubtedly related to changing oxygenation, redox mineralization, and organic-matter preservation, these relationships cannot be adequately explained. Pyritization of fossils and the abundance of pyrite nodules influence the amount of sulphur and may disturb the TOC to S relationship. Caution is required here, though, because the density of samples with both TOC and ICP data vary and the apparent variations may be because of the available data density.

DISCUSSION

Indicators of Anoxia and Organics

The whole-rock inorganic geochemical composition of marine sediments records a complex interplay between detrital debris and seawater-derived material (Goldberg, 1963). In the Haynesville Shale and Bossier Formation, the elements acquired here fall into three broad categories: those associated with siliciclastic terrestrial input (detrital debris of Goldberg [1963], Groups 1 and 3 in Figure 6), those associated with carbonates (Group 2 in Figure 6), and those associated with authigenic enrichments in oxygen-depleted sedimentary facies (seawater-derived material of Goldberg [1963], Group 5 in Figure 6).

The EFV values depicted in Figure 5 indicate that enrichment of vanadium and associated elements owing to a shift in deep-basin redox was prevalent during deposition of the Haynesville Shale (Package 3). This is particularly evident in the lower Haynesville Shale section of the wells in Texas (Glaspie, Georgetown 885 2, T.W. George, Carthage, and Watson) and throughout all of the Haynesville Shale section in the Louisiana wells (Williams, Hall 5, Elm Grove and Johnson Trust).

Where TOC values are high, there are corresponding high EFV values (Figure 5). High EFV is a typical feature of a starved, anoxic depositional facies (Tribovillard et al., 2006), a depositional environment proposed here for Package 3. This interpretation is supported by the low values of Th/U in Package 3, implying low terrigenous input and high organic contents. There are areas where EFV is high and TOC is not, possibly indicating there were no organics available in that area to be preserved.

Another common contributor to basinal black shale sediments are biota derived from the surface waters, with periods of high surface productivity being recorded by increased biotic debris in the sediments. In terms of the elemental data, this information can be modelled using P_2O_5, which, as discussed previously, is thought to be a proxy for biogenic apatite. High P_2O_5 values are recognized in several intervals of the Haynesville Shale, notably near the unit 3.1/3.2 boundary, the 2.2/2.3 boundary and the 2.4/ transition zone boundary (Figure 2). These P_2O_5 enrichments may be recording higher biogenic apatite, presumably derived from the surface waters. Therefore, the high P_2O_5 values are hypothesized to reflect deposition during periods of high surface productivity in the basin, as such, they are potentially coeval over relatively large distances. This is supported by the finding of abundant faecal pellets (comprised of calcareous nannoplankton) within areas of the Haynesville Shale (Spain and Anderson, 2010). Caution is required, however, because apatite is soluble in reducing waters and apatite can also be associated with periods of low depositional rates and condensed sequences (=bone beds).

Isochemical Maps

This study includes ten wells spanning a roughly west-east section throughout the basin. With this range of wells, it is possible to develop isochemical maps based on a number of geochemical characteristics. These maps delineate the average amount of, for example, CaO throughout the basin at a particular time, in this case the Haynesville Shale interval (Package 3). The values between the wells are interpolated based on the values at each well point. Because of this interpolation, isochemical maps are more representative between closely spaced wells.

We have created two isochemical maps (Figure 7), one showing V/Al_2O_3 values and the other showing Th/U values. As discussed previously, an enrichment in vanadium, which is seen here as high V/Al_2O_3 values, indicates reducing conditions that led to authigenic enrichment of V in the sediment (Tribovillard et al., 2006). Th/U is indicative of terrigenous content versus organic contents. The first map shows V/Al_2O_3 increasing gradually from west to east implying that dysoxic to anoxic bottom water conditions persisted for longer and were more pronounced in the Haynesville Shale section deposited in the eastern side of the study area. The Th/U values indicate high organic matter contents accumulated in areas where anoxia was developed and higher terrigenous inputs existed in the NW areas, implying that these areas were more proximal to a terrestrial sediment source.

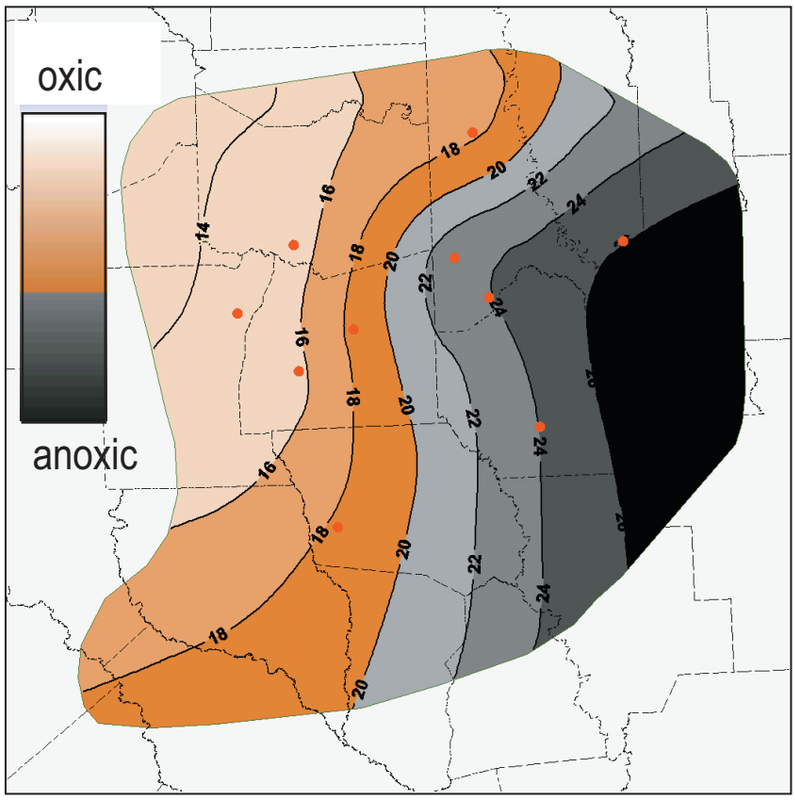

V/Al_2O_3

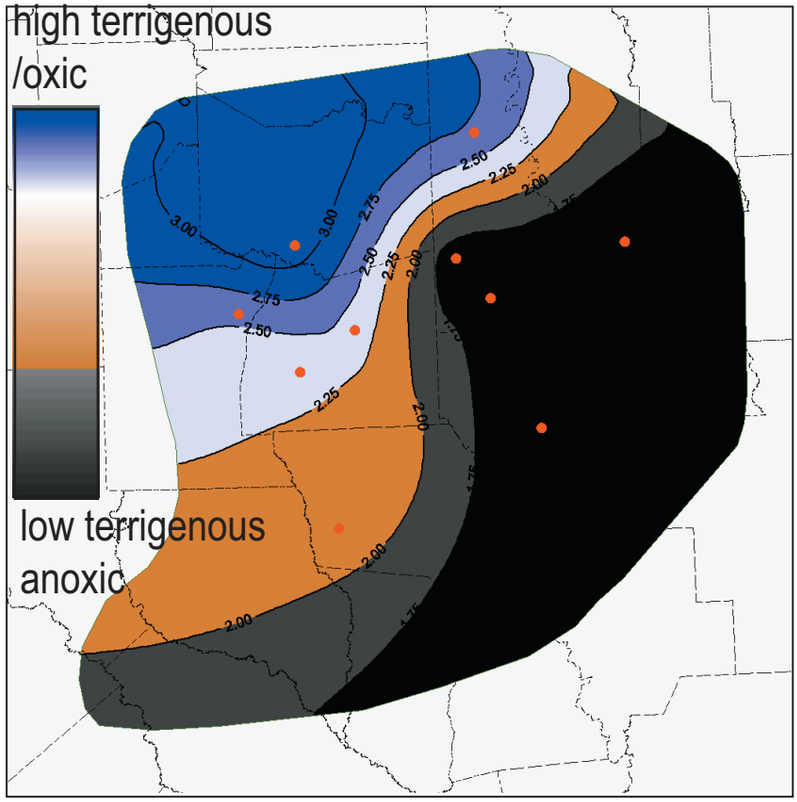

Th/U

Figure 7. Isochemical maps showing average V/Al_2O_3 values and Th/U values throughout the basin during the Haynesville Shale interval (Package 3). Red dots indicate the location of wells in the study. The values between the wells are interpolated based on the values at each well point.

Geochemical Trends and Cycles

In the previous sections, changes in the whole-rock geochemistry were used to identify chemostratigraphic packages and geochemical units that are broadly isochemical. However, it is also apparent that within the study interval some elements and element ratios show overall trends and fluctuations.

Depositional Trends

SiO_2 and Al_2O_3 values display consistent trends throughout the basin. These values are low at the top of Package 1, gradually increasing upward in Package 2, reaching a maximum in Package 3, and remaining high through the rest of this package (Figure 2). SiO_2 and Al_2O_3 both decrease in Package 4 and increase to very high values in Package 5. CaO displays an antithetic relationship to SiO_2 and Al_2O_3. Assuming that SiO_2 and Al_2O_3 are terrestrially derived and CaO is not, as discussed previously, these trends indicate that the amount of terrigenous sediment increases through the Gilmer Lime into the Haynesville Shale and on into the Bossier Formation suggesting an overall regressive sequence, although, as discussed later, lower order cycles are developed within this trend.

The Rb/K_2O ratio also displays distinct stratigraphic trends across the basin. The values of this ratio increase to a maximum at, or close to, the top of Unit 3.2 in all study wells (e.g., Figures 2, 5). From this point, the ratio decreases to a minimum in Package 4 and remains low in Package 5. As discussed fully previously, the mineralogical and geological controls on the Rb/K_2O ratio remain undetermined, but its variation appears to be stratigraphically controlled.

Cyclical Fluctuations

Figure 8 demonstrates that within Packages 1–4, the Zr/Nb ratio shows cyclical fluctuations. The controls on the Zr/Nb values suggested previously should be linked with the sediment coarseness, the high values of the ratio associated with siltier/sandier intervals, and the low values with clay-prone intervals. As such, it can be inferred that upward increasing Zr/Nb values are coarsening-up sequences and upward decreasing values upward fining-up sequences.

Typically, an upward coarsening interval is used to define an upward shoaling sequence terminating in a maximum regressive surface (MRS) and a fining upward sequence a transgressive sequence, culminating in a maximum regressive surface (MFS) (Donovan, 2010; Embry, 2010 and references cited therein). Therefore, the highest values (coarsest sediment) of Zr/Nb correspond to an MRS and lowest to an MFS. Figure 9 displays the resultant correlation between select wells when MRS and MFS are defined using Zr/Nb values. The resultant correlation implies that regressive portions of the cycles are better developed in the east than in the west, where terrigenous content is high and transgressive portions of the cycles are better developed in the east where terrigenous content is low, but organic content is high and anoxia was most severe. It also suggests that at least one regressive cycle is absent, or much thinned in the east of the basin. Furthermore, it indicates that the sedimentary facies exhibiting greatest evidence of anoxia are associated with initial transgression above an MRS, with evidence for anoxia decreasing toward the overlying MFS.

CONCLUSIONS

Inorganic whole-rock geochemical data enable a robust, largely objective chemostratigraphic correlation framework be proposed for the Smackover—Haynesville—Bossier study interval. With the chemostratigraphic zonation of the basin defined in this study, it is now possible to place any newly drilled well into this scheme, thereby removing the ambiguity that revolves around lithostratigraphic nomenclature in the basin. Furthermore, the geochemical data enable a refined correlation within the Haynesville Shale and provide a means to recognize and correlate transgressive—regressive sequences and, therefore, maximum flooding and maximum regressive surfaces. Combining the chemostratigraphic package and unit correlation with the definition of MFS and MRS provides a higher resolution correlation of the Haynesville Shale than is available from other, more traditional stratigraphic techniques. The correspondence between chemostratigraphic packages, geochemical units, and MFS/MRS correlation indicates that the suggested correlation is a close approximation to a chronostratigraphic correlation in the basin.

The same data used to define stratigraphic correlations can also be used to demonstrate:

- Terrigenous input into the basin displays an overall from the Gilmer Lime, through the Haynesville Shale into the Bossier Formation, with a short lived decrease at the top of the Haynesville Shale (Package 4).
- Throughout deposition of the Haynesville Shale, highest terrigenous input was in the NW portion of the basin.
- Throughout deposition of the Haynesville Shale, most severe anoxia existed in the south and east of the basin, suggesting that this region would have higher TOC values.

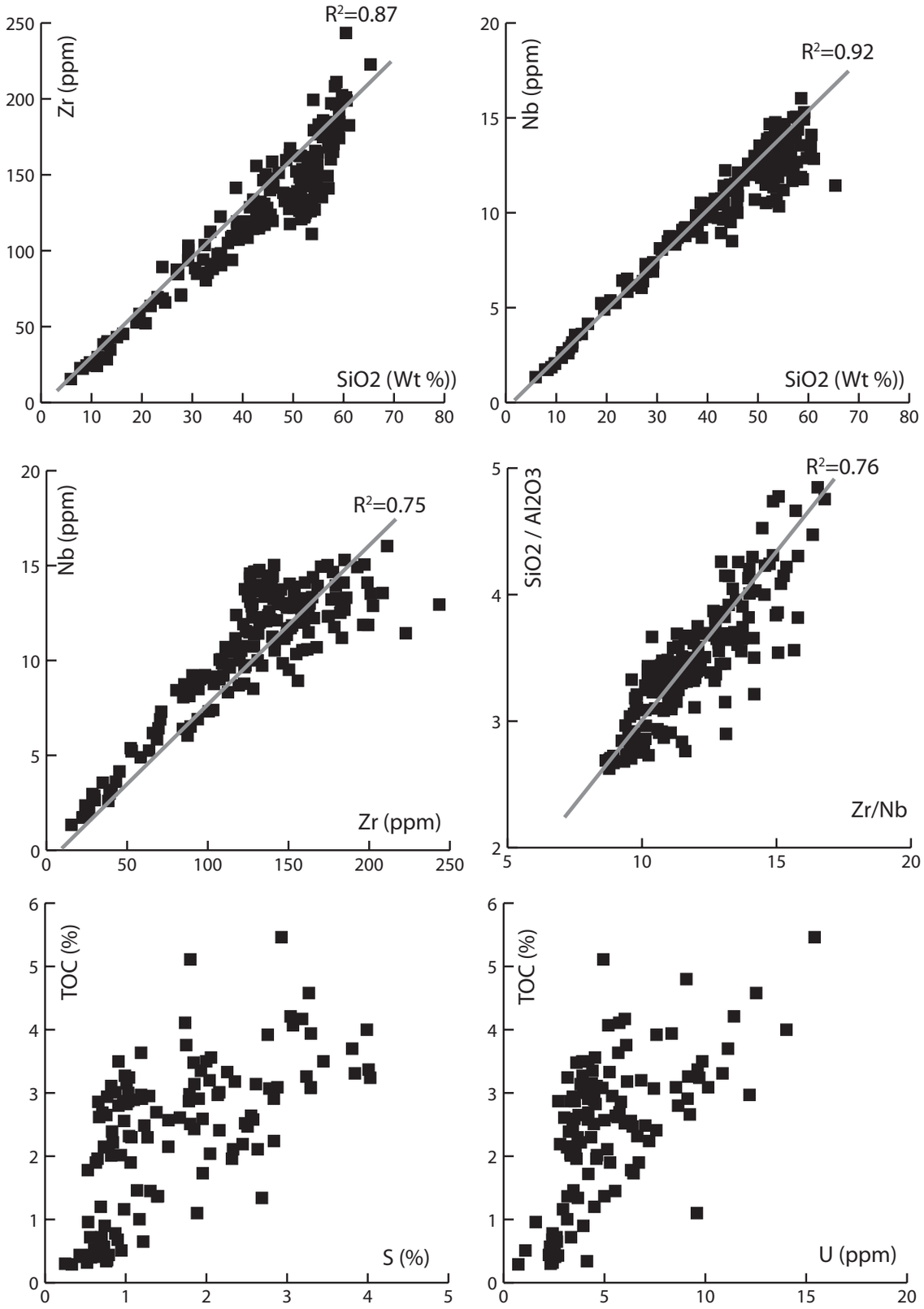

Figure 8. Selected element cross-plots demonstrating the relationships between Zr, Nb, SiO_2, Al_2O_3, U, S, and total organic carbon (TOC).

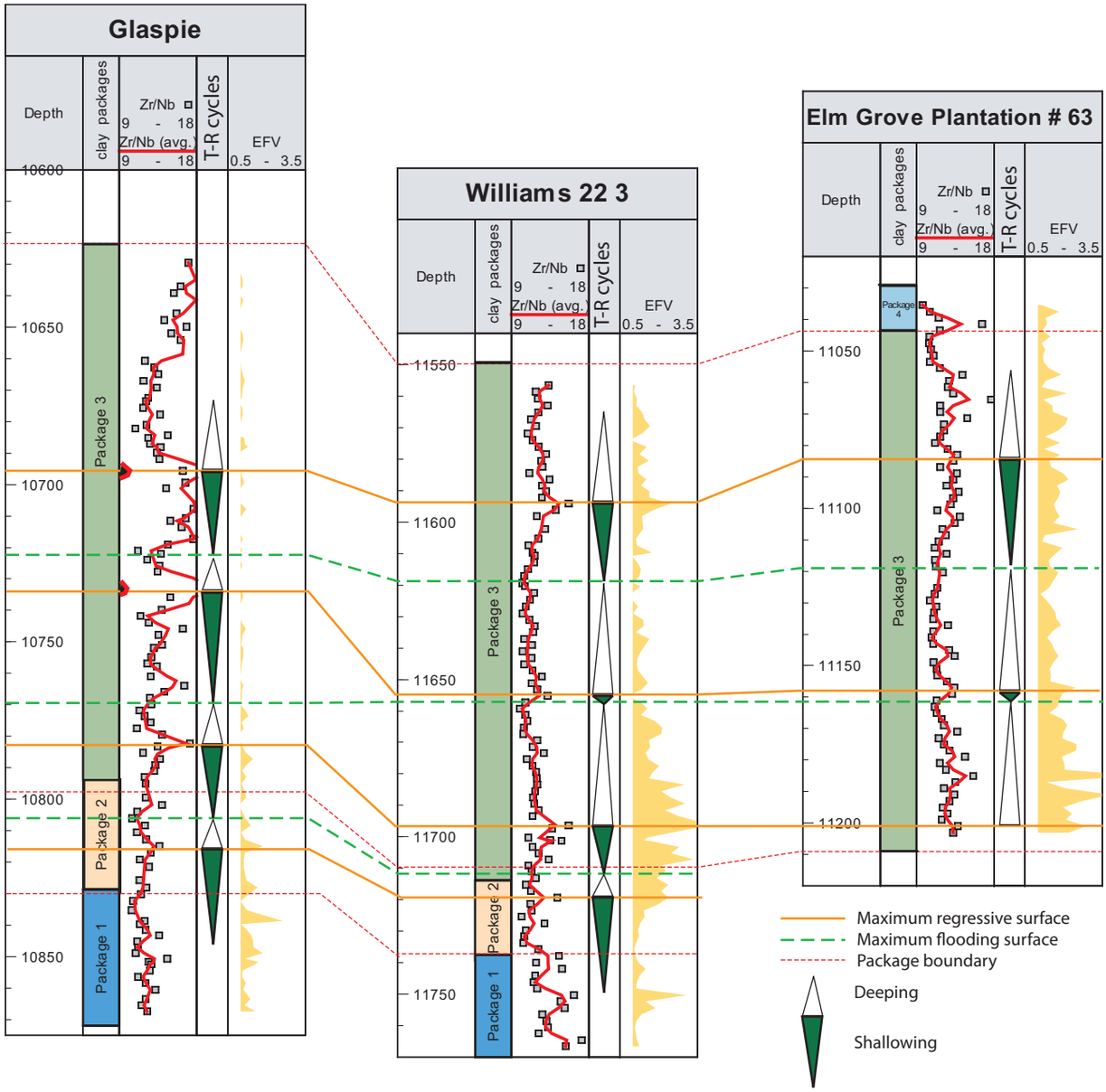

Figure 9. Zr/Nb chemical log showing repetitive fluctuations within Packages 1, 2, and 3 (left) and their interpretation in terms of base level fluctuation. Enrichment Factor of Vanadium (EFV) is shown to demonstrate parts of the succession that have facies that were deposited under anoxic conditions. For the Zr/Nb log, squares are the raw data and the solid line is a moving average with n = 2.

- Within the Haynesville Shale, greatest anoxia is always associated with the oldest defined transgressive sequence and maximum and evidence for anoxia occurs at the base of the transgressive sequence. This transgressive cycle thins to the west, resulting in little anoxia in the easterly wells.
- High TOC values are restricted to wells in the south and east of the basin and to the oldest transgressive cycle in the Haynesville Shale, providing a predictive tool for shale gas exploration in the Haynesville/Bossier Basin.

Although recognizing that each shale resource plays will differ, the general principles of using elemental geochemistry to define stratigraphic frameworks and to make inferences about basin anoxia laterally and temporally within a basin can readily be

applied to any shale interval in North America, as well as to other plays emerging globally.

ACKNOWLEDGMENTS

The authors would like to thank BP for allowing publication of the data pertaining to the study, Chemostrat Inc. for allowing the time and providing the support needed to prepare the manuscript, and Dave Wray and Lorna Dyer of The University of Greenwich at Medway in the UK for preparing and analyzing the samples on the ICP OES and MS. We would also like to acknowledge the contributions of core samples from operators who wish to remain anonymous. We extend our gratitude to Ellington and Associates in Houston, Texas, by whom the X-ray fluorescence and X-ray diffraction work was done, to Milly Wright of Chemostrat Inc. for her significant contributions to the manuscript and diagrams, and to Mike Dix, Simon Hughes, and Nicolo Casarta for their technical support of this study. Finally, we appreciate the editorial feedback from Dr. Harry Rowe and an anonymous reviewer, which led to significant improvements in the manuscript.

REFERENCES CITED

Cicero, A.D., I. Steinhoff, T. McClain, K.A. Koepke, and J.D. Dezelle, 2010, Sequence stratigraphy of the Upper Jurassic mixed carbonate/siliciclastic Haynesville and Bossier Shale depositional systems in East Texas and Northern Louisiana: Gulf Coast Association of Geological Societies Transactions, v. 60, p. 133–148.

Dix, M., D. Spain, C. Walling, J. Sano, N. Casarta, and A. Richardson, 2010, Stratigraphy and depositional dynamics of the Hayneville-Bossier sequence: Inferences from whole-rock elemental data: AAPG, Annual Convention & Exhibition, April 11–14, New Orleans, Louisiana, 2010.

Donovan, A., 2010, The sequence stratigraphy family tree: Understanding the portfolio of sequence methodologies, *in* K.T. Ratcliffe and B.A. Zaitlin, eds., Application of modern stratigraphic techniques: Theory and case histories SEPM SP PUB, no. 94, p. 5–33.

Ellwood, B.B., J.H. Tomkin, K.T. Ratcliffe, A.M. Wright, and A.M. Kafafy, 2008, Magnetic susceptibility and geochemistry for the Cenomanian/Turonian boundary GSSP with correlation to time equivalent core: Palaeo3, v. 251, p. 1–22.

Embry, A.F. 2010, Correlation siliciclastic successions with sequence stratigraphy, *in* K.T. Ratcliffe and B.A. Zaitlin, eds., Application of modern stratigraphic techniques: Theory and case histories SEPM SP PUB, no. 94, p. 35–53.

Forgotson, J.M., and J.M. Forgotson, Jr., 1976, Definition of Gilmer Limestone, Upper Jurassic Formation, northeastern Texas: AAPG Bulletin, Geologic Notes, 1119 p.

Goldberg, E.D., 1963. Mineralogy and chemistry of marine sedimentation, *in* F.P. Shepard, ed., Submarine geology: Harper & Row, New York, p. 436–466.

Goldhammer, R.K., and C.A. Johnson, 1999, Middle Jurassic-Upper Cretaceous paleogeographic evolution and sequence-stratigraphic framework of the northwest Gulf of Mexico rim, *in* C. Bartolini, R.T. Buffler, and A. Cantu-Chapa, eds., The western Gulf of Mexico Basin: Tectonics, sedimentary basins, and petroleum systems: AAPG Memoir 75, Tulsa, Oklahoma, p. 45–81.

Hammes, U., S.H. Hamlin, and R. Eastwood, 2010, Facies characteristics, depositional environment, and petrophysical characteristics of the Haynesville and Bossier shale-gas plays of East Texas and northwest Louisiana: Houston Geological Society Applied Geoscience Conference (AGS) of U.S. Gulf Coast Region, Mudstones as Unconventional Shale Gas/Oil Reservoirs, Houston, Texas, February 2010.

Hildred, G.V., K.T. Ratcliffe, A.M. Wright, B.A. Zaitlin, and D.S. Wray, 2010, Chemostratigraphic applications to low-accommodation fluvial incised-valley settings; an example from the Lower Mannville Formation of Alberta, Canada: Journal of sedimentary research, v. 80, p. 1032–1045.

Jarvis, I., and K.E. Jarvis, 1995, Plasma spectrometry in earth sciences: Techniques, applications and future trends, *in* I. Jarvis and K.E. Jarvis, eds., Plasma spectrometry in Earth Sciences: Chemical Geology, v. 95, p. 1–33.

Jenkyns, H.C. 2010. Geochemistry of oceanic anoxic events: Geochemistry Geophysics Geosystems, v. 11, p. 1–30.

Kimura, H., and Y. Watanabe, 2001, Oceanic anoxia at the Precambrian-Cambrian boundary: Geology, v. 29, no. 11, p. 995–998.

Negri, A., A. Ferretti, T. Wagner, P.A. Meyers, 2009, Organic-carbon-rich sediments through the Phanerozoic; processes, progress, and perspectives: Palaeogeography, Palaeoclimatology, Palaeoecology, v. 273, p. 302–328.

Pearce, T.J., D.S. Wray, K.T. Ratcliffe, D.K. Wright, and A. Moscariello, 2005, Chemostratigraphy of the Upper Carboniferous Schooner Formation, southern North Sea, *in* J.D. Collinson, D.J. Evans, D.W. Holliday, and M.S. Jones, eds., Carboniferous hydrocarbon geology: The southern North Sea and surrounding onshore areas: Yorkshire Geological Society, Occasional Publications series, v. 7, p. 147–164.

Pe-Piper, G., S. Triantafyllidis, and D.J.W. Piper, 2008, Geochemical identification of clastic sediment provenance from known sources of similar geology; the Cretaceous Scotian Basin, Canada: Journal of Sedimentary Research, v. 78, p. 595–607.

Ratcliffe, K.T., A.D. Hughes, D.E. Lawton, D.S. Wray, F. Bessa, T.J. Pearce, and J. Martin, 2006, A regional chemostratigraphically-defined correlation framework for the late Triassic TAG-I in Blocks 402 and 405a, Algeria: Petroleum Geoscience, v. 12, p. 3–12.

Ratcliffe, K.T., A. Morton, D. Ritcey, and C.E. Evenchick, 2007, Whole-rock geochemistry and heavy mineral analysis as exploration tools in the Bowser and Sustut basins, British Colombia, Canada: Bulletin of Canadian Petroleum Geology, v. 55, p. 320–337.

Ratcliffe, K.T., A.M. Wright, P. Montgomery, A. Palfrey, A. Vonk, J. Vermeulen, and M. Barrett, 2010, Application of chemostratigraphy to the Mungaroo Formation, the Gorgon field, offshore Northwest Australia: Australian Petroleum Production and Exploration Association, Journal, 50th Anniversary Issue, p. 371–388.

Rowe, H., and P. Manali, this volume, Chemostratigraphy and Paleoceanography of the Late Jurassic Haynesville-Bossier System, East Texas Basin: AAPG Bulletin v. 95.

Shaw, P.J.A., 2003, Multivariate Statistics for the environmental sciences, London: Hodder Arnold, 233.

Spain, D.R. and G.A. Anderson, 2010, Controls on reservoir quality and productivity in the Haynesville Shale, northwestern Gulf of Mexico Basin: Gulf Coast Association of Geological Societies Transactions, v. 60, p. 657–668.

Stevens, S., and Kuuskraa V., 2009, Seven plays dominate North America activity: Oil and Gas Journal, v. 107, n. 36, p. 39–49.

Svendsen, J., H. Friis, H. Stollhofen, and N. Hartley, 2007. Facies discrimination in a mixed fluvio-eolian setting using elemental whole-rock geochemistry—applications for reservoir characterisation: Journal of Sedimentary Research, 77, p. 23–33.

Tribovillard, N., T. Algeo, T.W. Lyons, and A. Riboulleau, 2006, Trace metals as paleoredox and paleoproductivity proxies; an update 2006: Chemical Geology, Vol. 232, Issue 1–2, p. 12–32.

Tribovillard, N., V.Bout-Roumazeilles, T. Algeo, T.W. Lyons, T. Sionneau, J.C. Montero-Serrano, A. Riboulleau, and F. Baudin, 2008. Paleodepositional conditions in the Orca Basin as inferred from organic matter and trace metal contents: Marine Geology, Vol. 254, Issue 1–2, p. 62–72.

Turgeon, S. and H.J. Brumsack, 2006, Anoxic vs. dysoxic events reflected in sediment geochemistry during the Cenomanian–Turonian boundary event (Cretaceous) in the Umbria–Marche Basin of central Italy: Chemical Geology v. 234, p. 321–339.

Wright, A.M., K.T. Ratcliffe, B.A. Zaitlin, and D.S. Wray, 2010a, The application of chemostratigraphic techniques to distinguish compound incised valleys in low-accommodation incised-valley systems in a foreland-basin setting: an example from the Lower Cretaceous Mannville Group and Basal Colorado Sandstone (Colorado Group), Western Canadian Sedimentary Basin, *in* K.T. Ratcliffe and B.A. Zaitlin eds., Application of modern stratigraphic techniques: Theory and case histories SEPM SP PUB, no. 94.

Wright, A.M., K.T. Ratcliffe, and D.R. Spain, 2010b, Application of inorganic whole rock geochemistry to shale resource plays: CURICP 10, 137946.